AD_____
(Leave blank)

Award Number: W81XWH-07-1-0596

TITLE: Nanovectors fo Targeting and Delivery of Therapeutics to HER-2/neu Positive Breast Cancer Cells

PRINCIPAL INVESTIGATOR: Rita E. Serda, Ph.D.

CONTRACTING ORGANIZATION:
University of Texas Health Science Center
HOUSTON, TX 77030

REPORT DATE: October 2008

TYPE OF REPORT: Annual

PREPARED FOR: U.S. Army Medical Research and Material Command
Fort Detrick, Maryland 21702-5012

DISTRIBUTION STATEMENT: (Check one)

√ Approved for public release; distribution unlimited

□ Distribution limited to U.S. Government agencies only; report contains proprietary information

REPORT DOCUMENTATION PAGE

Form Approved
OMB No. 0704-0188

1. REPORT DATE *(DD-MM-YYYY)*	**2. REPORT TYPE**	**3. DATES COVERED** *(From - To)*
10-14-2008	Annual report	15 Sep 2007 – 14 Sep 2008

4. TITLE AND SUBTITLE
Nanovectors fo Targeting and Delivery of Therapeutics to *
HER-2/neu Positive Breast Cancer Cells

5a. CONTRACT NUMBER
W81XWH-07-1-0596

5b. GRANT NUMBER
W81XWH-07-1-0596

5c. PROGRAM ELEMENT NUMBER

6. AUTHOR(S)
Rita Serda and Mauro Ferrari
Email: Rita.Serda@uth.tmc.edu

5d. PROJECT NUMBER

5e. TASK NUMBER

5f. WORK UNIT NUMBER

7. PERFORMING ORGANIZATION NAME(S) AND ADDRESS(ES)
UNIVERSITY OF TEXAS HEALTH SCIENCE CTR
1825 Pressler 537
HOUSTON, TX 77030

8. PERFORMING ORGANIZATION REPORT NUMBER

9. SPONSORING / MONITORING AGENCY NAME(S) AND ADDRESS(ES)
US Army Medical Research
820 Chandler Street
Fort Detrick MD 21702-5014

10. SPONSOR/MONITOR'S ACRONYM(S)
ARMY/MRMC

11. SPONSOR/MONITOR'S REPORT NUMBER(S)

12. DISTRIBUTION / AVAILABILITY STATEMENT
Distribution unlimited

13. SUPPLEMENTARY NOTES

14. ABSTRACT

Nanofabricated devices designed to carry drug and contrast agents to breast cancer cells are surface modified with targeting moieties that recognize unique or abundantly expressed molecules on the surface of tumor cells. However, major obstacles such as enzymatic degradation, uptake by professional phagocytes and the reticular endothelial system, and the vascular endothelium could hinder the ability of nanoparticles to reach the tumor site. To overcome these biological barriers, we have developed a multistage delivery system comprised of biocompatible porous silicon particles that encapsulate iron oxide nanoparticles for protection and transport to tumor-associated vasculature for magnetic resonance imaging of the tumor cell.

15. SUBJECT TERMS
None provided.

16. SECURITY CLASSIFICATION OF:			**17. LIMITATION OF ABSTRACT**	**18. NUMBER OF PAGES**	**19a. NAME OF RESPONSIBLE PERSON**
a. REPORT	**b. ABSTRACT**	**c. THIS PAGE**		25	**19b. TELEPHONE NUMBER** *(include area code)*

Standard Form 298 (Rev. 8-98)
Prescribed by ANSI Std. Z39.18

Table of Contents

Page

NANOVECTORS FOR TARGETING AND DELIVERY OF THERAPEUTICS TO HER-2 NEU POSITIVE BREAST CANCER CELLS

Serda, Rita E

INTRODUCTION

While our vast knowledge of cellular biology and genetics gives us insight into the mechanisms underlying uncontrolled cancer cell growth, it has yet to provide us with the key to selectively wipe out cancer cells. Current treatment with chemotherapeutic agents, administered either orally or intravenously, effectively poisons cancer cells, but also simultaneously attacks our healthy dividing cells. Encapsulation of therapeutic agents in delivery vectors reduces side effects and increases the half life of the drug. Delivery vectors can to engineering to specifically recognize tumor associated vasculature or tumorgenic breast epithelial cells. Our approach is to create multi-stage delivery vectors with different stages being capable of recognizing sequential biological barriers as they are unveiled. For example, tumor associated endothelial cells express elevated levels of VEGFR-2 receptor which can be targeted with antibodies (or aptamers) attached to the first stage of the delivery vector. Markers with increased expression on the surface of tumor cells, such as SUM225, CD44v6, and HER2, serve as targets for anchoring secondary stage particles, such as iron oxide or liposomal nanoparticles. HER-2 is a tumor-associated antigen which is overexpressed in 30% of all human breast cancers. The use of anti-HER2 antibodies is a well established and FDA approved method for the treatment of HER2 positive breast cancer. Herceptin (trastuzamab, Genetech, San Francisco, CA) is a recombinant DNA-derived humanized monoclonal antibody that selectively targets the extracellular portion of the human epidermal growth factor receptor 2 protein (HER2), making this a great marker for targeting the tumor.

BODY

The initial two aims of the project proposed to *1) validate binding of anti- HER2 /neu (hereafter HER2) antibody and antibody mimic to HER2 on human MCF-7/COX-2 breast cancer cells, and 2) to conjugate HER2 antibody or antibody mimic to the surface of iron oxide nanoparticles, as well as load porous silicon particles with iron oxide nanoparticles*. MCF-7 human breast cancer cells were phenotyped by flow cytometry and were found to express low levels of HER2 on their surface (fig. 1a), as previously published. The MCF-7/COX-2 model was not available for testing, therefore SKBR3 human breast

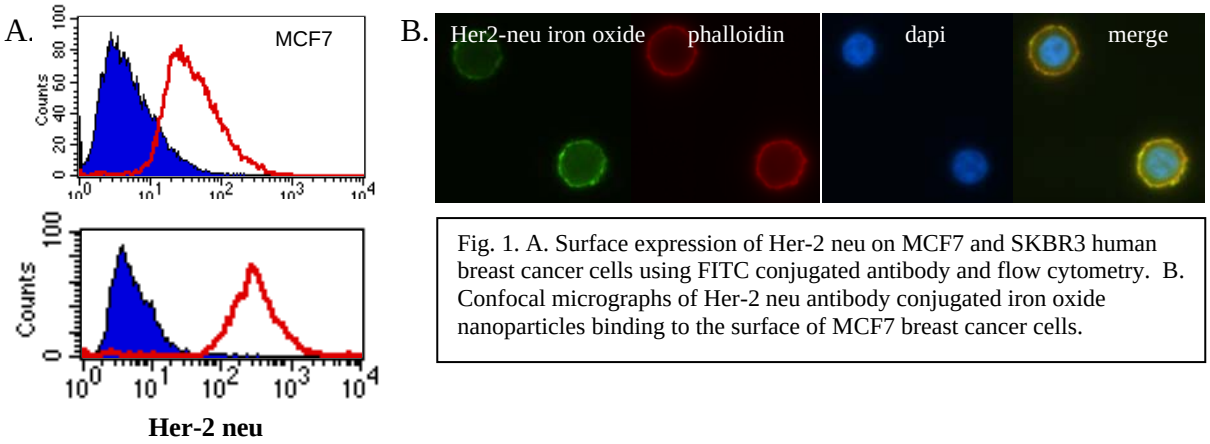

Fig. 1. A. Surface expression of Her-2 neu on MCF7 and SKBR3 human breast cancer cells using FITC conjugated antibody and flow cytometry. B. Confocal micrographs of Her-2 neu antibody conjugated iron oxide nanoparticles binding to the surface of MCF7 breast cancer cells.

cancer cells were tested for HER2 expression. The SKBR3 cell line was established from a pleural effusion. SKBR3 cells have amplified HER2, express EGFR and are ER-negative. As expected, HER2 expression on the surface of SKBR3 cells (fig. 1A) was strong. Thus we have two *in vitro* models with different degrees of HER2 expression to quantitate the effect of HER2 surface expression on binding and uptake of antibody targeted nanoparticles. The bivalent cyclic antibody mimic against Her-2 neu, (i.e. a peptide derived from the antigen-binding site of anti-Her-2 neu mAb) was proposed as a possible alternative to using the Her-2 neu antibody as the recognition ligand conjugated to iron oxide nanoparticles. This alternative has not been tested yet due to the high affinity and specificity demonstrated by the HER2 antibody.

The high research use and excellent targeting capabilities of HER2 antibody for nanoparticles delivery has lead to commercially available HER2 antibody conjugated iron oxide nanoparticles. The ability of these targeted nanoparticles to recognize HER2-expressing cells was tested with MCF-7 cells. Even with the low level of HER2 expression on the surface of these cells there was ample binding of the nanoparticles to the cells, as analyzed by fluorescent microscopy (fig. 1B).

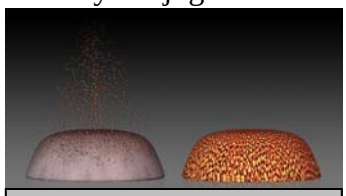

Fig. 2. Schematic showing iron oxide nanoparticles being loaded into porous silicon microparticles.

Various techniques were used to load iron oxide nanoparticles into porous silicon microparticles (fig. 2), including loading by capillary action, electrostatic attraction, and covalent attachment. Capillary action loading included loading microparticles overnight and loading with a small volume of concentrated iron oxide nanoparticles. Figure 3.A. shows a schematic of a microparticle and illustrates the angle of the slice used to generate the adjacent images, with the deeper cut on the right side of the particles providing an internal view of the pores in the microparticles. An electron micrograph showing the entire particle slice is shown in Figure 3.B., with a higher magnification image of the pores shown in Figure 3.C. While the microparticle shown in Figures "B" and "C" is unloaded, the microparticle in "D" is loaded with iron oxide nanoparticles which can be seen in the pores (pores are 30-40 nm in diameter, while iron oxide nanoparticles are 10 nm).

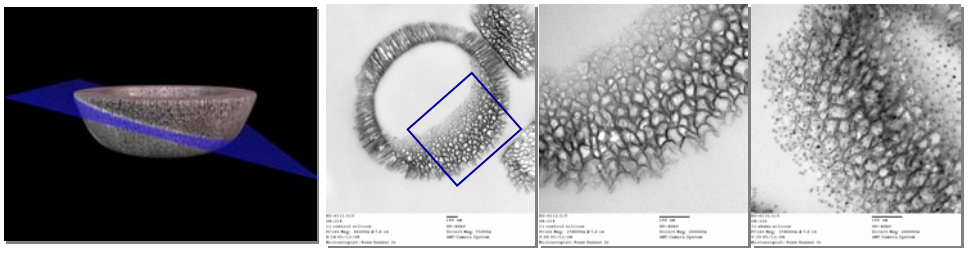

Figure 3. Loading iron oxide nanoparticles into pSi microparticles by capillary action. A. Schematic showing how the particles were cut for analysis. B-D. Transmission electron micrographs of unloaded (B,C) and iron oxide loaded (D) pSi microparticles.

Both electrostatic loading and covalent attachment of iron oxide nanoparticles into pSi microparticles resulted in abundant external attachment of iron oxide, however penetration into the pores was limited to the outer regions of the pore. Figure 4A is a scanning electron micrograph of a pSi microparticle covalently loaded with iron oxide nanoparticles.

Aim 3 proposed to image physical interactions of pSi microparticles to human vascular endothelial cells and monitor binding and internalization of iron oxide nanopartilces to human breast cancer cells. Initial studies aimed at validating the biocompatibility of the pSi microparticles with endothelial cells. Using Human Umbilical Vein Endothelial Cells (HUVEC) as a model, the growth of endothelial cells in the presence of microparticle was evaluated. Cells were grown for 72 hrs in either control media or with microparticles at a ratio of 5 microparticles to every one cell. PSi microparticles were either unloaded or loaded with either 10 nm iron oxide or 6 nm gold nanoparticles (Fig. 4B). Cell proliferation was measured by determining mitochondrial enzyme reduction of MTT (3-(4,5-dimethylthiazol-2-yl)-2,5-diphenyltetrazolium bromide, a tetrazole). The presence of microparticles, either loaded or unloaded with secondary nanoparticles did not affect cell growth. Other studies performed include live cell imaging studies showing microparticles undergoing mitosis with as many as 20 microparticles in a single cell (not shown).

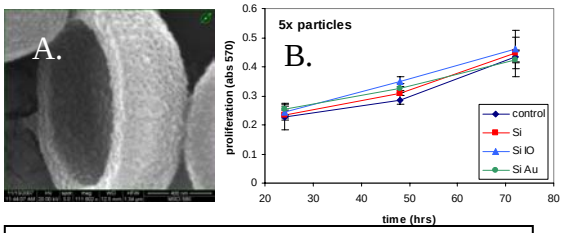

Fig. 4. A) Scanning electron microscope image of a porous silicon microparticle loaded with iron oxide nanoparticles (Si-IO). B) MTT proliferation assay showing normal growth of HUVECs in the presence of Si-IO.

PSi microparticles bind to the surface of HUVECs at 4ºC and are rapidly internalized at 37ºC. The scanning electron micrograph in Figure 5.A. shows a cell that is wrapped in pseudopodia extending from the cell. Contact of the particle with receptors on the cell membrane stimulates the cell to form an actin cup (fig. 5.B.) which wraps around the particle, completely enclosing the particle in a vesicle known as a phagosome. Cell uptake of particles is actin dependent, as confirmed by experiments in which cytochalasin B blocked uptake of particles (not shown, however included in the enclosed manuscript). This supports a role for phagocytosis as the mechanism by which particles are internalized.

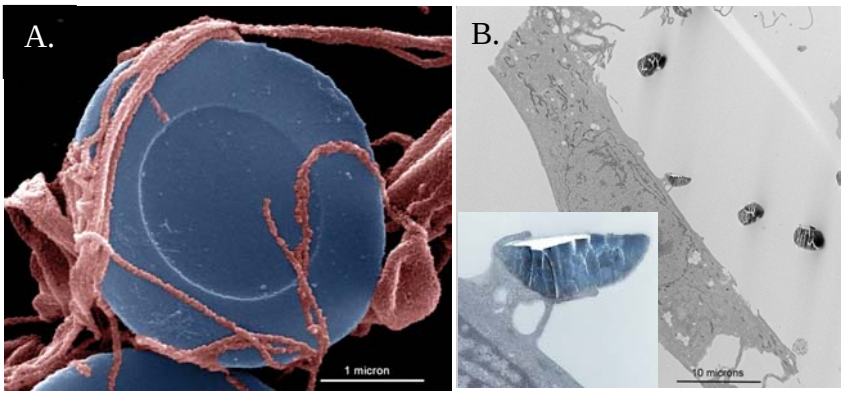

Figure 5. Psuedo-colored electron microgarphs show pSi microparticles being engulfed by HUVEC endothelial cells. A. Scanning electron micrograph shows pseudopodia wrapped around a pSi particle. B. Transmission electron micrographs show formation of an actin cup during microparticle uptake (images represents cells that have been incubated in media containing microparticles for 30 minutes at 37ºC).

While pSi microparticles are rapidly internalized by HUVECs in serum-free media, they are discriminately internalized in the presence of serum opsonins. Opsonization of pSi microparticles inhibited uptake of negatively charged oxidized particles, but had no effect on uptake on positively charged (APTES modified) particles (data included in enclosed manuscript). Opsonins present in the blood that bind to negatively charged pSi particles block binding to receptors on the surface of HUVECs that are needed for particle

internalization. We also find that pure IgG binding to particles inhibits cell uptake, indicating that IgG binding from serum may be a major opsonin responsible to decreased cell uptake. This is interesting as it is the same process that increases uptake of particles by macrophages. The data makes sense with respect to expression of Fc gamma receptors on the surface of the two cell types. Macrophages express high levels of these receptors while expression is absent or negligible on HUVECs.

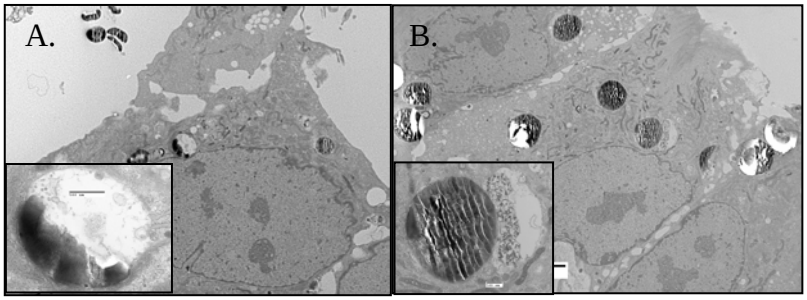

Figure 6. Transmission electron micrographs showing intracellular location of 1.5 µm (A.) or 3.0µm (B) microparticles in HUVEC endothelial cells after 120minutes of incubation in serum-free media at 37ºC.

Once internalized the early fate of microparticles is dictated by their size. The smaller microparticles (1.5 µm) are internalied in vesicles (fig. 6.A.), while the larger (3 µm) microparticles lack a clear membane enclosure and appear to be located in the cytoplasm (fig. 6.B.). At later time points all the microparticles appear to be located in the cytoplasm (data not shown). More studies are currently underway to determine the intracellular location of these particles and the means by which they escape the phagosome.

Aim 4 proposed image in vivo trafficking of silicon nanovectors and iron oxide nanoparticles in a xenograft model of human breast cancer by MR imaging and monitor cytotoxicity of iron oxide nanoparticles due to thermal ablation. Human breast cancer xenografts were established in nude mice by injection of 1 x 10^5 4T1 human breast cancer cells into the mammary fatpad of female 5-6 week old Crl Fox^{nu} nude mice. After 2 weeks, either saline, iron oxide nanoparticles (50 µg), or 1 x 10^8 silicon microparticles (1.6 µm), loaded with iron oxide nanoparticles, were intraveneously administered via tail vein injection. Magnetic resonance imaging was carried out using a 7 Telsa magnetic resonance imager. Coronal slices, shown in Figure 7, show accumulation of the contrast agent (Fe) within the tumor 3 hrs post injection for both the free iron oxide nanoparticles and those enclosed in pSi microparticles. Both iron and silicon content in the tissues was determined using inductively coupled plasma mass spectroscopy (data not shown).

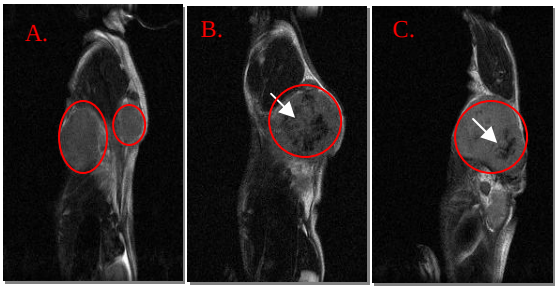

Fig. 7. MRI coronal slices of a human breast tumor developed in a mouse mammary fat pad (3 hr post injection of either saline (A), iron oxide nanoparticles (B), or porous silicon microparticles loaded with iron oxide nanoparticles (C). Tumors are circled and location of contrast argent is marked by arrows.

After imaging, blood was collected from the mice and mononuclear cells were isolated using Ficoll-paque™ density centrifugation. The scanning electron micrograph in Figure 8A contains 4 macrophages and a smaller lymphocyte. The pseudo-colored image on the right (Fig. 4B) displays a macrophage whose shape suggests internalization of one or more silicon microparticles. Figure 8C is a high magnification micrograph of a macrophage.

All *in vivo* experiments performed to date have been with non-targeted particles. Future experiments will focus on sequential *in vivo* targeting of tumor-associated endothelium by first-stage silicon microparticles, followed by tumor specific targeting with second-stage iron oxide nanoparticles. As stated previously, HER2-conjugated iron oxide nanoparticles and VEGFR-2 antibody (or aptamer) conjugated particles pSi microparticles will be used for multistage targeting. endothelial cells will be explored by *in vitro* and *in vivo* techniques.

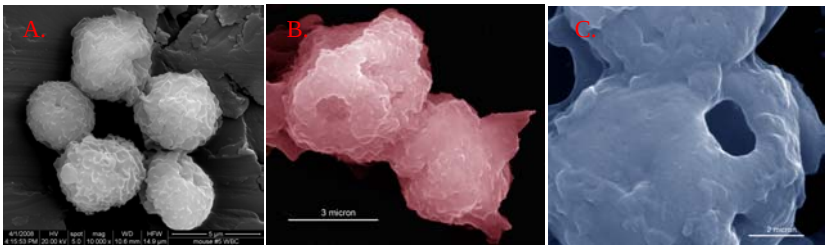

Fig. 8. Scanning electron micrographs of mouse blood cells 2 hrs after intravenous injection of multistage particles. Note: images B and C are false-colored.

KEY RESEARCH ACCOMPLISHMENTS

- Characterization of HER2 expression on breast cancer cell lines and acquisition of HER2 antibody conjugated iron oxide nanoparticles
- Confirmation of binding of HER2 antibody conjugated nanoparticles to MCF-7 breast cancer cells in culture by fluorescent microscopy
- Loading of porous silicon (pSi) microparticles with iron oxide nanoparticles (multistage delivery system)
- Demonstrated biocompatibility of multistage delivery system with endothelial cells (MTT assay)
- Demonstrated endothelial cell internalization of pSi microparticles by transmission and scanning electron microscopy and established mechanism of uptake to be phagocytosis
- Determined the effect of pSi microparticle size and charge on uptake by endothelial cells
- Determined the effect or serum and IgG on uptake of microparticles by endothelial cells
- Performed initial *in vivo* animal experiments with the non-targeted multistage delivery system with visualization of biodistribution by magnetic resonance imaging

REPORTABLE OUTCOMES

Manuscripts

Serda RE, Gu J, Bhavane RC, Liu X, Chiappini C, Robertson FM, Decuzzi P, Ferrari M. Microengineering delivery vectors to target inflamed vascular endothelium and reduce uptake by the reticulo-endothelial system. Submitted.

Godin B, Gu J, **Serda RE**, Liu X, Tanaka T, Decuzzi P, Ferrari M. Tailoring the degradation kinetics of mesoporous silicon structures though PEGylation, submitted.

Chapters and Non-peer reviewed Articles

Serda R, Robertson F, Ferrari M. Overcoming nature's fastball - Bio-barriers in cancer nanotechnology. *Nano the Magazine for Small Science*, Issue 5, 010-013, Jan 2008.

Serda R, Chiappini C, Fine D, Tasciotti E, Ferrari M. Chapter: Porous silicon particles for imaging and therapy of cancer. Kumar (Ed.): Nonmagnetic Inorganic Nanomaterials for Life Sciences (NmLS Vol.2), WILEY-VCH Verlag GmbH & Co. Submitted June 2008.

Poster Presentations

Nanoporous silicon delivery vectors for breast cancer imaging. **Serda RE**, Godin B, Gu J, Bankson J, Decuzzi P, Ferrari M. *BMES Annual Meeting 2008, Fall 2008, St. Louis MI.*

Multistage delivery systems for the imaging and therapy of breast cancer. **Serda RE**, Bhavane R, Cheng M, Liu X, Robertson F, Decuzzi P, Ferrari M. *Department of Defense Era of Hope, Summer 2008, Baltimore, MD.*

Stealth silicon vehicles: controlled phagocytosis of silicon microparticles by HUVEC. **Serda R**, Bhavane R, Cheng M, Liu X, Robertson F, Decuzzi P, Ferrari M. *University of Texas Health Science Center at Houston Research Day 2007, Fall 2007, Houston, TX.* ***(NOTE: FIRST PLACE AWARD)***

INVENTIONS

Invention Title : Microengineering mesoporous silicon particles for opsonization directed uptake by endothelial cells
Invention Docket Number: 2008-0057
Invention Report Number: 0578417-08-0014
Primary Agency: ARMY/MRMC Invention
Report Date: 09/23/2008
Invention Status: Under Evaluation

CONCLUSION

Phagocytosis of silicon microparticles (i.e. delivery vectors) by both endothelial cells and macrophages is sensitive to serum opsonization of the microparticles. While silicon microparticles are indiscriminately taken up by both endothelial cells and macrophages in serum-free media, serum opsonization leads to selective uptake of microparticles. Thus it is possible to microengineer delivery vectors to drive binding to specific serum components, thereby directing interaction of microparticles with tumor-associated endothelium while simultaneously avoiding uptake by the reticular endothelial system, without the aid of targeting ligands. These delivery vectors have been successfully loaded with iron oxide nanoparticles, which serve as contrast agents for magnetic resonance imaging (MRI). We have shown that it is possible to track the location of the iron oxide loaded pSi microparticles in animal models of human breast cancer by MRI. Future experiments will focus on specifically targeting intravenously administered nanoparticles and microparticles to bypass sequential barriers in the body; microparticles will be engineered to associate with tumor-associated endothelium while nanoparticles are engineered to bind to and be internalized by breast cancer epithelial cells. Targeted particles should preferentially localize within the tumor for imaging by MRI. With time the porous silicon particles degrade with kinetics dependent upon the pore size.

APPENDICES

- manuscript

Welcome: ANNALISE MARTIN
Office of Technology Transfer Administra
UNIVERSITY OF TEXAS HLTH SCI CTR HOUSTO

Invention Report Search

Choose "Add Patent Report" to add a new patent report to the selected invention report. Choose "Modify Invention Report
selected invention report.

Results for Invention Report Search

Invention Title	**Microengineering mesoporous silicon partilces for opsonization directed upt endothelial cells**			
Invention Docket Number	2008-0057	Invention Report Number	0578417-08-0014	
Primary Agency	ARMY/MRMC	Invention Report Date	09/23/2008	Add Patent Modify Inve
Invention Status	Under Evaluation			

Return to Search Screen

Microengineering delivery vectors to target inflamed vascular endothelium and reduce RES uptake

Rita E. Serda[1*], Jianhua Gu[1], Rohan C. Bhavane[1], Xuewu Liu[1], Ciro Chiappini[2], Fredika M. Robertson[3], Paolo Decuzzi[4, 5], Mauro Ferrari[*, 1, 3, 6]

[1]University of Texas Health Science Center, Department of Biomedical Engineering, Nanomedicine Division, 1825 Pressler, Suite 537, Houston, TX 77030; [2]University of Texas at Austin, Department of Biomedical Engineering, 1 University Station, C0400, Austin, TX 78712; [3]University of Texas MD Anderson Cancer Center, Department of Therapeutics, Unit 422, 1515 Holcombe Blvd., Houston, TX 77030; [4]Universita' degli Studi Magna Græcia, Viale Europa, Italy; [5]School of Health Information Sciences, University of Texas Health Science Center Houston, 7000 Fannin, Houston, TX 77030; [6]Rice University, Department of Bioengineering, Houston, TX 77005;

Manuscript information

Number of text pages: 14

Number of figures: 6

Number of tables: 0

Abbreviations: RES – reticulo-endothelial system**;** PEG - poly(ethylene glycol); APTES - 3-aminopropyltriethoxysilane; HUVEC – human umbilical endothelial cells; CSF-1 – colony stimulating factor; FcR – Fc receptor; , IgG - immuno gamma globulin; FD – FITC dextran; CB – Cytochalasin B

[*]**To whom correspondence should be addressed: Mauro Ferrari and Rita Serda**

Department of Biomedical Engineering, Nanomedicine Division

University of Texas Health Science Center

1825 Pressler Street, Suite 537

Houston, TX 77030

Phone: 713-500-3941; Email: Mauro.Ferrari@uth.tmc.edu; Rita.Serda@uth.tmc.edu

ABSTRACT

Chronic inflammation is associated with many pathological lesions, including cancer and atherosclerosis. Inflammatory cytokines stimulate the expression of adhesion molecules and cell surface receptors on endothelial cells and drug delivery vehicles can be microengineered to target those receptors. Here we show that nanoporous silicon delivery vehicles are phagocytosed by both endothelial cells and macrophages. Under serum-free conditions microparticles are internalized nondiscriminately, however, in the presence of serum, uptake is dependent upon expression of opsonin receptors, which varies by cell population. Opsonized amine modified silicon microparticles were rapidly internalized by endothelial cells; and this uptake was enhanced following cytokine stimulation. On the other hand, serum opsonization inhibited endothelial uptake of oxidized microparticles by 78%. This blocking action was greater than the shielding effect provided by a surface layer of poly (ethylene glycol). Conversely, macrophages displayed a preference for internalization of opsonized oxidized microparticles. This cell type dependent preference was also seen for the internalization of oxidized microparticles opsonized with pure IgG. IgG opsonization increased internalization of oxidized microparticles by macrophages by 35-47%, while inhibiting uptake by endothelial cells by 76-88%. Therefore, rather than using polymers to block opsonization, microparticles can be surface engineered to direct opsonization that favors uptake by target populations.

INTRODUCTION

Acute inflammation promotes healing by fighting infections and injury; however, chronic inflammation can be detrimental. In addition to pathologies including atherosclerosis and vasculitis, chronic inflammation contributes to tumor initiation, progression and development of metastases (1). During inflammation, immune cells secrete cytokines which increase expression of adhesion molecules on vascular endothelial cells and attract leukocytes (2-4). Cytokines such as TNF-α also stimulate expression of COX-2 by tumor cells which produces pro-inflammatory lipids and supports angiogenic growth, further exacerbating tumor growth (5;6).

Nano- and micro-sized delivery systems are emerging as powerful tools for the systemic delivery of therapeutic molecules and imaging agents for different biomedical applications, from cancer (7;8) to cardiovascular diseases (9). Following intravenous injection, these particles are transported by the blood stream into different vascular districts. Targeting diseased vasculature is a strategy already demonstrated to be effective for the detection of atherosclerotic plaque and cardiovascular alterations (10;11), and it is becoming more prominent in cancer applications (12;13). Typically, delivery vectors are conjugated with ligand molecules that specifically recognize and interact with receptors uniquely or over-expressed at the vascular targeting site. Targeting ligands include peptides identified from phage-displayed libraries (14), thioaptamers (15), and antibodies. A downside of this strategy is that ligand molecules, such as antibodies, are generally immunogenic, leading to prompt recognition of the particles by professional phagocytes. Attempts at bypassing phagocytic uptake by shielding with polymers, such as poly(ethylene glycol), successfully prolongs circulation time, but limits attachment of targeting ligands to the particle (16).

While it is well established that professional phagocytes play a role in macromolecular uptake (17), it is also recognized that vascular endothelial cells can ingest micron-sized particulates by phagocytosis (18;19). Signals for phagocytosis include surface antigens and serum components (opsonins) which cover the particulate's surface. Receptors for opsonins include Fc receptors (FcR), complement receptors, adhesion molecules, and scavenger receptors. Due to selective expression of surface receptors on different cell populations, opsonins differ for each population of phagocytic cells (20).

We have recently developed a silicon-based microparticle with a nanoporous structure (8). These microparticles are characterized by a quasi-hemispherical shape which enhances lateral migration of the microparticles (21), thus increasing the likelihood of vascular recognition (21). In this work, we demonstrate that surface properties of nanoporous silicon microparticles can be engineered to favor opsonization with serum components that enhance interaction of microparticles with inflamed endothelium while delaying uptake by macrophages. Directed uptake of microparticles by serum opsonization bypasses the need for PEGylation, which favors prolonged circulation time but interferes with attachment of targeting ligands and subsequent interaction of these ligands with cell surface receptors (16).

METHODS

Silicon Particle Fabrication. Nanoporous hemispherical silicon microparticles were designed, engineered, and fabricated in the Microelectronics Research Center at The University of Texas at Austin. Two sizes of microparticles were generated, with mean diameters of 1.6 and 3.2 μm, and pore sizes ranging from 5-10 nm. Processing details were recently published by our laboratory (8) and are described in more detail in the supplemental material.

Surface Modification of Silicon Microparticles. Silicon microparticles were dried and then treated with piranha solution (1 volume H_2O_2 and 2 volumes of H_2SO_4) at 110-120 ^{0}C for 2 hr. Particles were then washed and incubated overnight in IPA containing 0.5% (v/v) APTES (Sigma). 3-aminopropyltriethoxysilane (APTES) modified microparticles were reacted with 10 mM mPEG-SCM-5000 (methoxy poly-ethylene glycol succinimidyl carboxymethyl; purchased from Laysan Bio Inc.) in acetonitrile for 1.5 hr. Microparticles were counted in a Z2 Coulter® Particle Counter and Size Analyzer (Beckman Coulter).

Cell Culture. HUVECs, purchased from Lonza Walkerville, Inc. (Walkersville, Maryland), were cultured in EBM®-2 medium (Clonetics®, CC-3156). For serum-free experiments, EBM®-2 medium (Clonetics®) was supplemented with only hydrocortisone and GA-1000, plus 0.2% BSA. J774 macrophage cells were purchased from American Type Culture Collection (Manassas, VA). Growth medium was Dulbecco's Modified Eagle's Medium containing 10% FBS, 100 µg/ml streptomycin and 100 U/ml Penicillin (Invitrogen; Carlsbad, CA).

Confocal Microscopy. HUVECs, grown on glass cover slips, were incubated with microparticles (10 microparticles per cell) for 60 min in serum-free media. Cells were then fixed and premeabilized with 0.1% triton x-100. PBS containing 1% BSA was used as a blocking agent prior to incubation with 200 nM Alexa Fluor 555 conjugated Phallodin (Invitrogen) and anti-tubulin FITC conjugated antibody (Abcam inc., Cambridge, MA). Vectashield mounting media (Vector Laboratories, Burlingame, CA), containing either DAPI or a 1000-fold dilution of DRAQ5 (Biostatus Limited, UK), was used for nuclear staining. Detection of silicon microparticles was based on either autofluorescence using a 633 excitation laser or modification of particles with Dylight-488 NHS ester (Pierce). Images were acquired using a Leica DM6000 upright confocal microscope equipped with a 63x oil immersion objective.

Flow Cytometry. HUVECs were incubated with either silicon microparticles (20 microparticles/cell) or Fluoresbrite® YG Microspheres (1:1000 ; 1 µm; Polysciences) in serum-free media, or as specified, for the indicated time at 37ºC. For opsonization experiments, microparticles were preincubated with either serum, BSA (4 g/dL in PBS), or ImmunoPure® Human Whole Molecule IgG (500 mg/dL; Pierce, Rockford, IL) on ice for 60 min. Cells were then washed with PBS, harvested by trysinization (HUVEC) or scrapping (J774), and resuspended in PBS containing 1.0% BSA and 0.1% sodium azide (FACS wash buffer). Microparticle association with cells was determined by measuring side scatter using a Becton Dickinson FACSCalibur Flow equipped with a 488-nm argon laser and CellQuest software (Becton Dickinson; San Jose, CA). Comparisons of FITC Dextran (0.5 mg/ml) internalization by HUVECs are based on fluorescent intensity measurements following incubation of cells with microparticles at 37ºC for 1 hr.

Expression of FcγRs was studied on HUVECs before and after stimulation with with TNF-α (10 ng/ml) and IFN-γ (100 U/ml) for 48 hrs. Flow cytometric analysis was performed on live cells, which were identified by their lack of propidium iodide staining. Antigen density calculations were based on a QuickCal® calibration curve generated with Quantum™ Simply Cellular® anti-Mouse IgG (Bangs Laboratories, Inc.; Fishers, IN). For inhibition studies, HUVECs were incubated in cytochalasin B (2.5, 5.0 and 10.0 µg/ml) for 60 min at 37ºC prior to addition of microparticles and during the 60 minute incubation with microparticles (1:20).

Scanning Electron Microscopy. HUVEC and J774 cells grown on 5 x 7 mm Silicon Chip Specimen Supports (Ted Pella, Inc., Redding, CA) were treated with microparticles (1:20) at 37ºC for the specified

amount of time. Samples were washed, fixed, dehydrated, and treated hexamethyldisilazane (Sigma). Specimens were mounted on SEM stubs (Ted Pella, Inc.) using conductive adhesive tape (12mm OD PELCO Tabs, Ted Pella, Inc.), and sputter coated with a 10 nm layer of gold using a Plasma Sciences CrC-150 Sputtering System (Torr International, Inc.). SEM images were acquired under high vacuum, at 20.00 kV, spot size 3.0-5.0, using a FEI Quanta 400 FEG ESEM equipped with an ETD (SE) detector.

Transmission Electron Microscopy. Microparticles were introduced at a cell to particle ratio of 1:20 at 37ºC for either 15 or 120 min. Cells were then processed for TEM analysis and examined in a JEM 1010 Transmission Electron Microscope (JOEL, USA, Inc., Peabody, MA) at an accelerating voltage of 80 kV. Digital images were obtained using the AMT Imaging System (Advanced Microscopy Techniques Cory, Danvers, MA).

RESULTS AND DISCUSSION

Effect of Surface Charges on Microparticle Uptake. Nanoporous silicon delivery vectors were fabricated using a porosification process developed by Ferrari and colleagues (22) involving photolithography. To examine the response of endothelial cells to silicon microparticles, two sizes of microparticles, 1.6 and 3.2 µm, and three types of surface modifications were explored. All experiments were performed with both sizes of microparticles in triplicate, and representative experiments are presented. Silicon microparticles were oxidized with a piranha solution to create negatively charged, hydroxylated microparticles. Complete surface oxidation was confirmed by energy dispersive spectrophotometer analysis (data not shown). Surface modification with APTES yielded positively charged, amine modified microparticles. APTES modified microparticles were further conjugated with mPEG-5000 to create shielded microparticles.

Using human umbilical vein endothelial cells (HUVECs) as a model for vascular endothelium, scanning electron microscope (SEM) images were taken of cells after incubation with microparticles. After one hour at 37ºC, both positive and negative microparticles were internalized by HUVECs in serum-free media (**Fig. 1A**). Surface modification of silicon microparticles with mPEG-5000 suppressed internalization of microparticles (**Fig. 1A**).

Serum Opsonization Inhibits HUVEC Uptake of Oxidized Silicon Microparticles. Several *in vivo* studies suggest that the pattern of opsonins adsorbed to the surface of particulates determines the population of phagocytic cells responsible for their clearance (23). For example, plasma protein adsorption by poly(D,L-lactic acid) nanoparticles enhances uptake by monocytes, while decreasing binding to lymphocytes (24). Leroux et al. (25) reported that opsonization of PEG-coated nanoparticles by serum proteins enhanced their uptake by monocytes, however, removal of IgG from the serum reduced uptake of PEG particles, indicating that PEG-coated particles are able to bind IgG components in the serum.

Cells containing internalized microparticles have an increase in granularity as demonstrated by

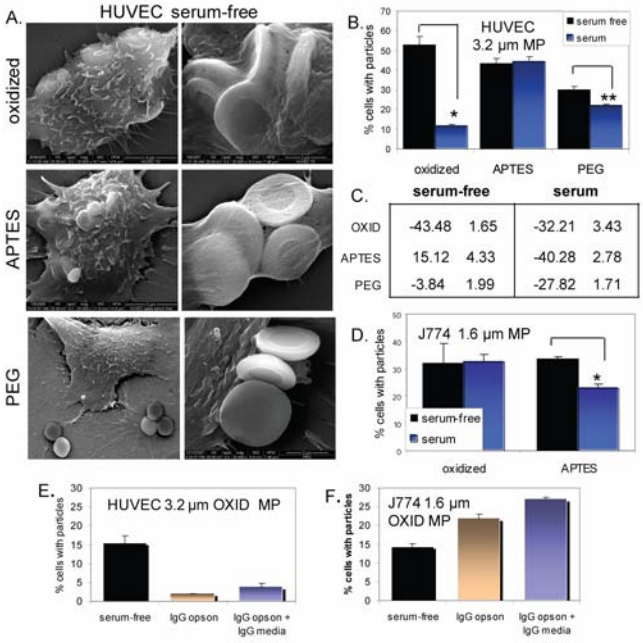

Figure 1.

an upward shift in orthogonal (90º) laser light scatter (side scatter) based on flow cytometric analysis. Using side scatter as a metric to determine the association of HUVECs with microparticles, the effect of serum on uptake of silicon microparticles was examined. Microparticles were opsonized in 100% fetal bovine serum for 60 min on ice, followed by incubation with HUVECs in the continued presence of 5% serum. Internalization of oxidized microparticles by HUVECs was strongly inhibited (78%), however serum opsonization failed to have an impact on internalization of APTES microparticles by HUVECs. Opsonization of PEG modified microparticles lead to a 27% decrease in uptake by HUVECs (**Fig. 1B**). To evaluate the generality of inhibition of uptake of negatively charged microparticles by endothelial cells following serum opsonization, negatively-charged polystyrene microparticles (Fluoresbrite® YG, 1 µm) were opsonized in serum, then incubated with HUVECs in media containing 5% serum. In the presence of serum, there was a 33-fold decrease in uptake of polystyrene microparticles, supporting the conclusion that serum blockade of internalization of negatively charged microparticles by vascular endothelial cells is a global phenomenon regardless of the type of microparticle used (**supplemental data Fig. 1**).

Surface charge, based on zeta potential measurements, was altered for oxidized, APTES and mPEG modified silicon microparticles following opsonization with serum (**Fig. 1C**). All opsonized microparticles had a negative surface charge. While the APTES and mPEG microparticles became more negatively-charged, the oxidized microparticles showed a decrease in negative charge (+11.27 mV).

Similar to endothelial cells, J774 mouse macrophages were able to take up positive and negative silicon microparticles non-discriminately in serum-free media (**Fig. 1D**). However, in the presence of serum, J774 cells were responsive to particle bound opsonsins. In contrast to HUVECs, J774 cells favored uptake of opsonized oxidized microparticles.

HUVECs express complement receptors, such as CR1 and CR4 (26). However, the C5a receptor, found on spleen, liver and lymphatic vessels, is not expressed by blood vessel endothelial cells (27). Selective expression of complement receptors may be one mechanism of targeting subpopulations of endothelial cells. To determine if activation of the complement system affected uptake of microparticles by HUVECs, oxidized microparticles were incubated with HUVECs following opsonization with serum or heat-inactivated serum. Active complement enhanced serum induced inhibition of microparticle uptake by 13% ($p = 0.0027$) (**supplemental data Fig. 2**). Physiological levels of albumin (4 g/dL), on the other hand, had no significant effect on internalization of particles (**supplemental data Fig. 2**), as has been previously reported (25).

There are three categories of Fc gamma receptors (FcγR), FcγRI/CD64, FcγRII/CD32, and FcγRIII/CD16. FcγRs are reported to be either absent or expressed at low levels on unstimulated endothelial cells (28-30). Although FcγRII expression has been found to occur on human placental endothelial cells, expression does not extend into the umbilical cord (31). To confirm this, we incubated HUVECs with antibodies specific for each category of FcγR. While HUVECs did not express appreciable levels of FcγRI and FcγRIII on their surface, there was low but detectable levels of FcγRII (**supplemental data Fig. 3**). Based on a calibration curve generated using Quantum™ Simply Cellular® microspheres, HUVECs express approximately 10,000 FcγRII per cell. J774 cells also failed to express FcγRI, but expressed both FcγRII and FcγRIII. Due to minimal expression of FcγRs by HUVECs, immuno gamma globulin (IgG) opsonization of microparticles could block binding and internalization of microparticles.

Arvidsson (32) showed rapid (1 min) binding of antibody specific for High Molecular Weight Kininogen (HMWK) to oxidized silicon immersed in plasma. To examine the ability of antibody opsonization to block binding of oxidized microparticles to HUVECs, microparticles were opsonized with ImmunoPure Human Whole Molecule IgG at 500 mg/dL. Uptake of IgG opsonized microparticles

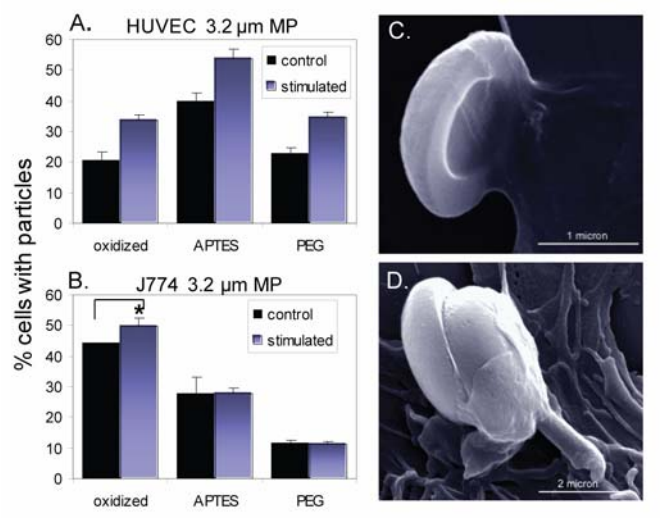

Figure 2.

HUVECs. Since it has been reported that activation of endothelial cells by pro-inflammatory cytokines induces surface expression of FcγRs (28), expression of FcγRs on HUVECs was examined following 48 hrs treatment with TNF-α (10 ng/ml) and IFN-γ (100 U/ml). Based on flow cytometric analysis, cytokine stimulation increased surface expression of FcγRII by HUVECs, with each cell expressing approximately 35,000 receptors per cell (**supplemental data Fig. 3**). Expression of FcγRII by stimulated J774 cells was similar to basal levels, with each cell expressing approximately 320,000 receptors.

Internalization of serum opsonized silicon microparticles by HUVECs was enhanced for all groups of microparticles following exposure to TNF-α and IFN-γ; however a clear preference for opsonized APTES microparticles continued to exist (**Fig. 2A**). Enhanced expression of FcγRII and adhesion molecules may mediate this increased uptake of microparticles. J774 cells continued to show a clear preference for opsonized oxidized microparticles, which was significantly enhanced (11%) in the presence of cytokines ($p = 0.045$) (**Fig. 2B**). Uptake of APTES and PEG modified microparticles by J774 cells was not affected by exposure to TNF-α and IFN-γ. Figure 2 contains SEM images displaying early uptake (15 min) of serum opsonized APTES and oxidized microparticles by HUVEC (**Fig. 2C**) and J774 (**Fig. 2D**) cells, respectively.

by HUVECs was strongly inhibited, regardless of whether free IgG was included in the media (76%) or not (88%) (**Fig. 1E**). This is in contrast to internalization of IgG opsonized microparticles by J774, which was enhanced by 35% and 47% in the absence or presence of free IgG, respectively (**Fig. 1F**). Internalization of APTES microparticles by HUVECs was unaffected by preincubation of microparticles with pure IgG (**supplemental data Fig. 4**).

Cytokine Stimulation Enhances Phagocytosis of Silicon Microparticles by

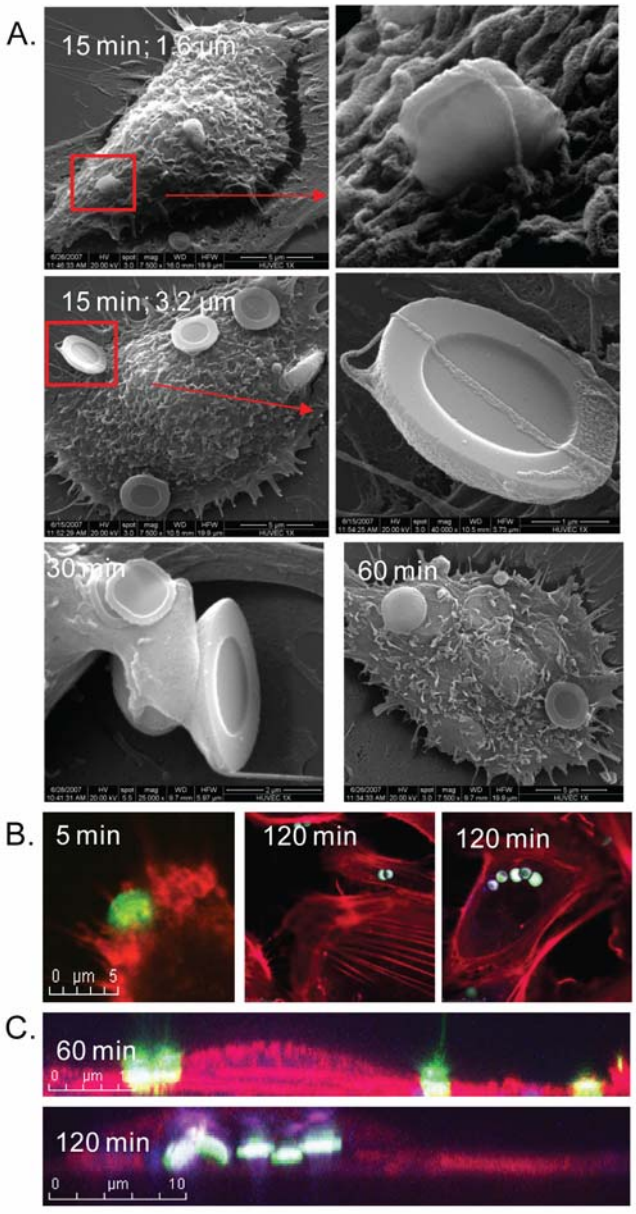

Figure 3.

Characterization of Silicon Microparticle Uptake by HUVECs. Since all opsonized silicon microparticles have negative surface charges, we used negatively charged oxidized silicon microparticles in serum-free media to evaluate the mechanism by which HUVECs internalize silicon microparticles. SEM experiments demonstrated that early contact (15 min, 37ºC) of HUVECs with microparticles induces formation of pseudopodia that extends outward to surround both 1.6 and 3.2 µm particles (**Fig. 3A**). SEM analysis at 30 min provided visual evidence that HUVECs were actively engulfing microparticles. After 60 min, a large number of microparticles are completely internalized by HUVECs which can be visualized beneath the plasma membrane. Confocal microscopy images, taken after 5 min of incubation of HUVECs with microparticles, verify the formation of membrane extensions by HUVECs reaching out to surround the microparticles (**Fig. 3B**). Microparticles are visualized based on autofluorescence, while the cell periphery (i.e. actin) is labeled with Alexa Fluor 555 conjugated Phalloidin. After 120 min, the microparticles were completely internalized. **Figure 3C** are confocal projection images cropped through the center of a z-series to illustrate the cellular location of the microparticles over time. Microparticles taken up at the cell periphery migrate toward the cell body and are localized in the perinuclear region after 120 min.

Cytochalasin B Blocks Uptake of Silicon Microparticles by HUVECs. Both phagocytosis and macropinocytosis are active processes that involve reorganization of the actin cytoskeleton leading to changes in the shape of the cell membrane that allow uptake of large particles and extracellular fluid. Cytochalasin B dissociates actin-binding protein from actin filaments, weakening existing actin filaments, and blocking actin polymerization (33). Therefore Cytochalasin B blocks uptake of particles by both phagocytosis and macropinocytosis. To confirm the involvement of actin polymerization in the uptake of silicon microparticles, HUVECs were pre-incubated with Cytochalasin B (2.5 µg/ml) for 60 min, then incubated with both 1.6 µm and 3.2 µm oxidized microparticles for 15-60 min (37ºC). SEM analysis at 15 min shows a lack of pseudopodia engaging microparticles which have settled on the cell surface (**Fig. 4A**). After 30 min, the HUVECs appear to have initiated actin cup formation, which is a dense actin network that forms beneath the microparticles (34), however, uptake is frustrated by Cytochalasin B, preventing internalization of the microparticles. In the absence of Cytochalasin B, further actin polymerization would induce expansion of the actin cup which would completely surround the microparticle, creating a phagosome.

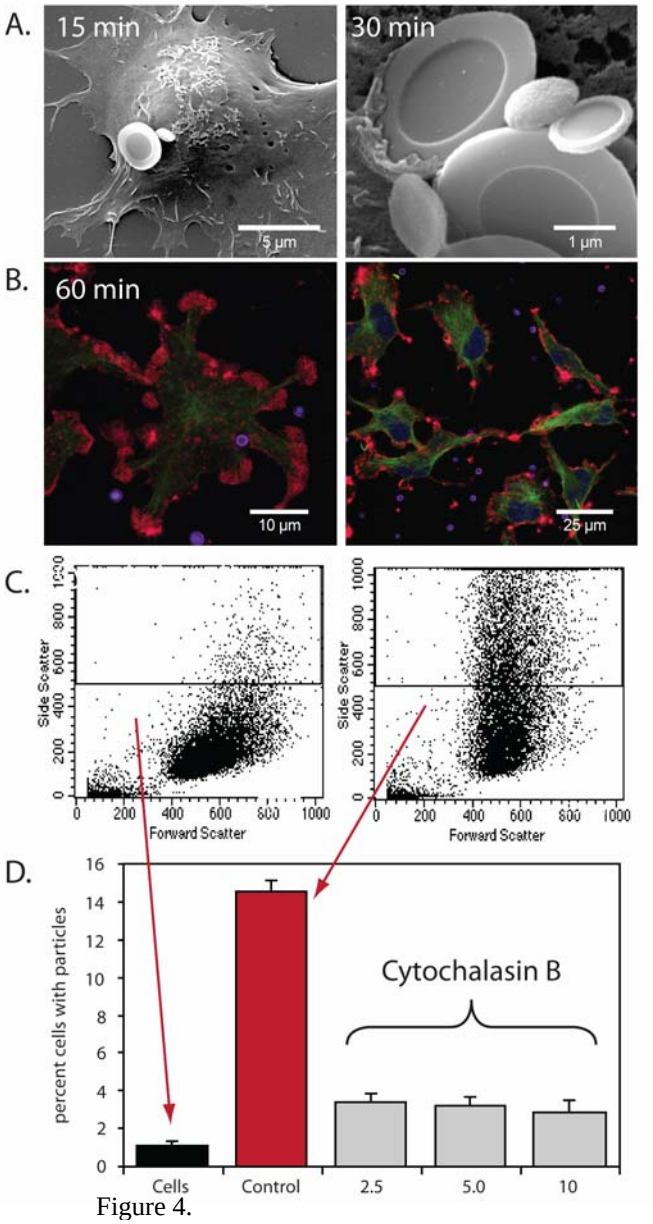

Figure 4.

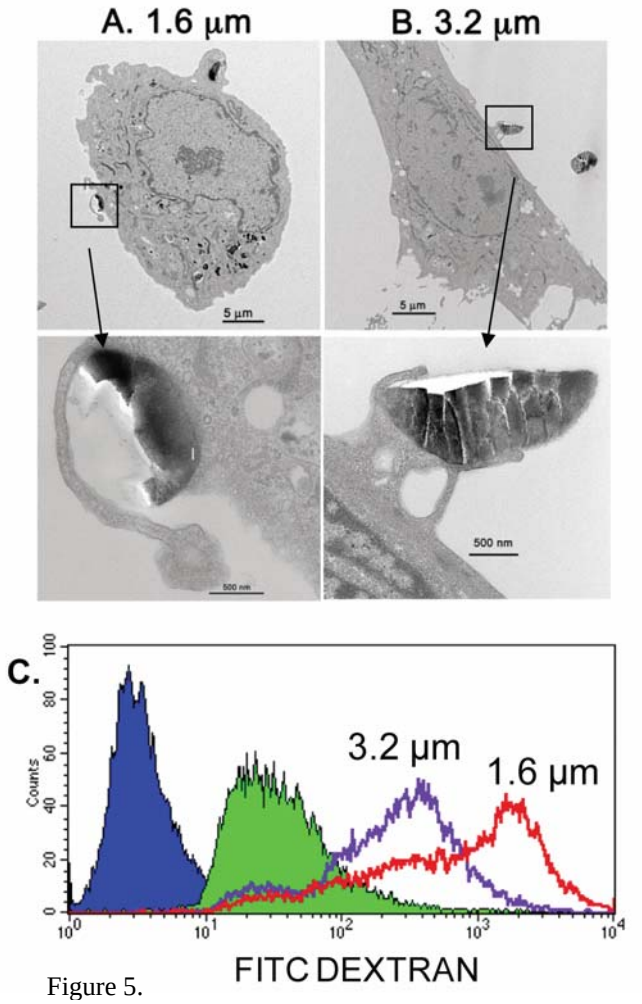

Figure 5.

Confocal images, taken after 60 min of incubation, support a lack of microparticle uptake by HUVECs in the presence of Cytochalasin B (**Fig. 4B**).

Based on flow cytometric analysis of side scatter (**Fig. 4C)**, dose dependent inhibition of microparticle uptake by Cytochalasin B was evaluated. Cytochalasin B, at concentrations of 2.5 µg/ml and higher inhibited microparticle uptake by HUVECs by 85-88% (**Fig. 4D**).

Effect of Microparticle Size on Phagocytosis/Macropinocytosis by HUVECs. Transmission electron microscopy (TEM) images of HUVECs incubated with microparticles for 15 min further demonstrate formation of pseudopodia in engulfment and uptake of both sizes of microparticles. In **Figure 5A**, the cell membrane has completely surrounded one of the microparticles with a diameter of 1.6 µm. In a separate region of the same cell, the membrane is engulfing a particle by what appears to be macropinocytosis. Macropinocytosis results in the bulk uptake of both fluid and solid cargo (35) and has previously been reported to occur in microvascular endothelial cells (36). Analysis of TEM imaging of the uptake of the larger 3.2 µm particles by HUVECs is consistent with classical phagocytosis, with the hallmark presence of an actin cup holding a microparticle (**Fig. 5B**).

Internalization of fluorescein isothiocyanate (FITC) dextran (FD) from the cell media is used to measure fluid uptake by cells (i.e. macropinocytosis). Flow cytometric analysis of FD internalization during microparticle uptake confirmed that there was a greater amount of FD associated with uptake of 1.6 µm particles compared to FD uptake with 3.2 µm particles, supporting a greater role for macropinocytosis in HUVEC uptake of 1.6 µm particles (**Fig. 5C**).

Intracellular Trafficking of Silicon Microparticles. TEM images of HUVECs incubated with 1.6 µm oxidized silicon microparticles for 2 hrs at 37ºC show microparticles located in the perinuclear region of the cell (**Fig. 6 A**). Trafficking of microparticles to the perinuclear region reflects movement towards the minus ends of microtubules and supports microtubule-based transport consistent with cargo

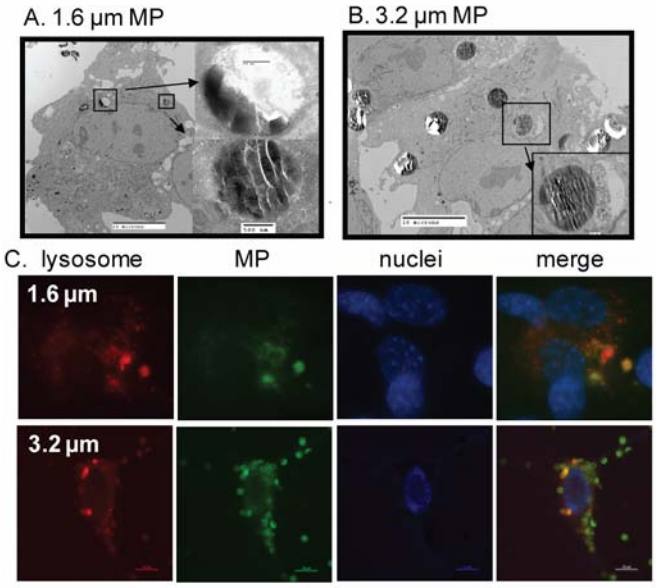

Figure 6.

delivery from early to late endosomes (37). Based on the spherical shape and the presence of multiple vesicular bodies in the transport vesicle housing the 1.6 μm particle (**Fig. 6A**), it is likely that the phagosome containing the microparticle undergoes a typical maturation to a late endosomal state containing multiple intraluminal vesicles. While some microparticles are clearly enclosed in membranes, it is unclear if other microparticles are similarly housed within vesicles. As shown in **Figure 6B**, the larger 3.2 μm particles are more disperse and the majority of microparticles show no evidence of membrane enclosure.

Slowing *et al.* (38) reported that human cervical cancer cells (HeLa) efficiently internalize mesoporous silica nanoparticles. They reported that the more negatively charged silica nanoparticles were able to escape from endosomes within 6 hrs, while the more positively charged particles remained trapped within endosomes. Our study supports the lack of apparent vesicular membranes surrounding the majority of the larger, oxidized 3.2 μm particles.

To further address the issue of intracellular location of microparticles, colocalization of microparticles with late endosomes or lysosomes was explored at 2 hrs using Lysotracker Red to stain acidic vesicles. APTES modified microparticles were labeled using DyLight 488 NHS ester prior to incubation with HUVECs. A large number of the smaller, 1.6 μm particles colocalized with acidic vesicles, however only a few of the 3.2 μm particles colocalized with acidic vesicles after 2 hrs (**Fig. 6C**). These data are consistent with the lack of an apparent vesicle membrane surrounding the majority of the larger 3.2 μm particles, suggesting cytoplasmic localization.

CONCLUSIONS

This research suggests that vascular targeting of endothelial cells is enhanced by serum opsonins that preferentially bind to positively charged microparticles. In contrast, serum opsonins binding to negatively charged microparticles strongly inhibit uptake by endothelial cells. Fortunately, professional phagocytes, such as macrophages, showed a preference for negatively charged opsonized microparticles. Perhaps opsonins binding to negatively charged microparticles are reflective of serum components which decorate bacteria and apopotic cells, both of which have a net negative surface charge and are targets for uptake by neutrophils and macrophages (39;40). Positively charged microparticle shielding with serum components, aka macrophage dys-opsonins, resists the need for PEGylation and concurrent compromised targeting. Microparticle internalization by endothelial cells is enhanced by pro-inflammatory cytokine stimulation, supporting superior uptake of positively charged microparticles at sites of chronic inflammation. Therefore, it is conceivable to microengineer particles to attract a regime of opsonins that support preferential targeting of endothelium associated with pathologies including coronary artery disease, vasculitis, and cancer.

REFERENCES

[1] Marx, J, Cancer research. Inflammation and cancer: the link grows stronger. *Science* 306 (2004) 966-968.

[2] Batten, P., Yacoub, M. H., Rose, M. L., Effect of human cytokines (IFN-gamma, TNF-alpha, IL-1 beta, IL-4) on porcine endothelial cells: induction of MHC and adhesion molecules and functional significance of these changes. *Immunology* 87 (1996) 127-133.

[3] Beekhuizen, H., van Furth, R., Monocyte adherence to human vascular endothelium. *J.Leukoc.Biol.* 54 (1993) 363-378.

[4] Smith, C. W., Endothelial adhesion molecules and their role in inflammation. *Can.J.Physiol Pharmacol.* 71 (1993) 76-87.

[5] Subbarayan, V., Sabichi, A. L., Llansa, N., Lippman, S. M., Menter, D. G., Differential expression of cyclooxygenase-2 and its regulation by tumor necrosis factor-alpha in normal and malignant prostate cells. *Cancer Res.* 61 (2001) 2720-2726.

[6] Robertson, F. M., Mallery, S. R., Bergdall-Costell, V. K., Cheng, M., Pei, P., *et al.*, Cyclooxygenase-2 directly induces MCF-7 breast tumor cells to develop into exponentially growing, highly angiogenic and regionally invasive human ductal carcinoma xenografts. *Anticancer Res.* 27 (2007) 719-727.

[7] Sakamoto, J., Annapragada, A., Decuzzi, P., Ferrari. M., Antibiological barrier nanovector technology for cancer applications. *Expert Opin. Drug Deliv.* 4 (2008) 359-369.

[8] Tasciotti, E., Liu, X., Bhavane, R., Plant, K., Leonard, A.D., *et al.*, Mesoporous silicon particles as a multistage delivery system for imaging and therapeutic applications. *Nature Nanotech.* 3 (2008) 151-157.

[9] Cyrus, T., Lanza, G. M., Wickline, S. A., Molecular imaging by cardiovascular MR. *J.Cardiovasc.Magn Reson.* 9 (2007) 827-843.

[10] Lanza, G., Winter, P., Cyrus, T., Caruthers, S., Marsh, J., *et al.*, Nanomedicine opportunities in cardiology. *Ann.N.Y.Acad.Sci.* 1080 (2006) 451-465.

[11] Kang, H. W., Torres, D., Wald, L., Weissleder, R., Bogdanov, A. A., Jr., Targeted imaging of human endothelial-specific marker in a model of adoptive cell transfer. *Lab Invest* 86 (2006) 599-609.

[12] Hu, G., Lijowski, M., Zhang, H., Partlow, K. C., Caruthers, S. D., *et al*, Imaging of Vx-2 rabbit tumors with alpha(nu)beta3-integrin-targeted 111In nanoparticles. *Int.J.Cancer* 120 (2007) 1951-1957.

[13] Hood, J. D., Bednarski, M., Frausto, R., Guccione, S., Reisfeld, R. A., *et al.*, Tumor regression by targeted gene delivery to the neovasculature. *Science* 296 (2002) 2404-2407.

[14] Arap, W., Haedicke, W., Bernasconi, M., Kain, R., Rajotte, D., *et al.*, Targeting the prostate for destruction through a vascular address. *Proc.Natl.Acad.Sci.U.S.A* 99 (2002) 1527-1531.

[15] Bassett, S. E., Fennewald, S. M., King, D. J., Li, X., Herzog, N. K., *et al.*, Combinatorial selection and edited combinatorial selection of phosphorothioate aptamers targeting human nuclear factor-kappaB RelA/p50 and RelA/RelA. *Biochemistry* 43 (2004) 9105-9115.

[16] Gabizon, A., Shmeeda, H., Horowitz, A. T., Zalipsky, S., Tumor cell targeting of liposome-entrapped drugs with phospholipid-anchored folic acid-PEG conjugates. *Adv.Drug Deliv.Rev.* 56 (2004) 1177-1192.

[17] Gordon, S., The macrophage: past, present and future. *Eur.J.Immunol.* 37 Supp l 1 (2007) S9-17.

[18] Beekhuizen, H., van de Gevel, J. S., Olsson, B., van, B., I, van, F. R., Infection of human vascular endothelial cells with Staphylococcus aureus induces hyperadhesiveness for human monocytes and granulocytes. *J.Immunol.* 158 (1997) 774-782.

[19] Ibrahim, A. S., Spellberg, B., Avanessian, V., Fu, Y., Edwards, J. E., Jr., Rhizopus oryzae adheres to, is phagocytosed by, and damages endothelial cells in vitro. *Infect.Immun.* 73 (2005) 778-783.

[20] Patel, H. M., Moghimi, S. M., Serum-mediated recognition of liposomes by phagocytic cells of the reticuloendothelial system - The concept of tissue specificity. *Adv.Drug Deliv.Rev.* 32 (1998) 45-60.

[21] Decuzzi, P., Lee, S., Bhushan, B., Ferrari, M., A theoretical model for the margination of particles within blood vessels. *Ann.Biomed.Eng* 33 (2005) 179-190.

[22] Cohen,M.H.,Melnik,K., Boiarski, A.A., Ferrari, M., Martin,F.J., Microfabrication of Silicon-Based Nanoporous Particulates for Medical Applications. Biomed. *5* (2003) 253-259.

[23] Borchard, G., Kreuter, J., The role of serum complement on the organ distribution of intravenously administered poly (methyl methacrylate) nanoparticles: effects of pre-coating with plasma and with serum complement. *Pharm.Res.* 13 (1996) 1055-1058.

[24] Leroux, J. C., Gravel, P., Balant, L., Volet, B., Anner, B. M., *et al.*, Internalization of poly(D,L-lactic acid) nanoparticles by isolated human leukocytes and analysis of plasma proteins adsorbed onto the particles. *J.Biomed.Mater.Res.* 28 (1994) 471-481.

[25] Leroux, J. C., De, J. F., Anner, B., Doelker, E., Gurny, R., An investigation on the role of plasma and serum opsonins on the internalization of biodegradable poly(D,L-lactic acid) nanoparticles by human monocytes. *Life Sci.* 57 (1995) 695-703.

[26] Langeggen, H., Berge, K. E., Johnson, E., Hetland, G., Human umbilical vein endothelial cells express complement receptor 1 (CD35) and complement receptor 4 (CD11c/CD18) in vitro. *Inflammation* 26 (2002) 103-110.

[27] Linehan, S. A., Martinez-Pomares, L., Stahl, P. D., Gordon, S., Mannose receptor and its putative ligands in normal murine lymphoid and nonlymphoid organs: In situ expression of mannose receptor by selected macrophages, endothelial cells, perivascular microglia, and mesangial cells, but not dendritic cells. *J.Exp.Med.* 189 (1999) 1961-1972.

[28] Pan, L. F., Kreisle, R. A., Shi, Y. D., Detection of Fcgamma receptors on human endothelial cells stimulated with cytokines tumour necrosis factor-alpha (TNF-alpha) and interferon-gamma (IFN-gamma). *Clin.Exp.Immunol.* 112 (1998) 533-538.

[29] Alberto, M. F., Bermejo, E. I., Lazzari, M. A., Receptor expression for IgG constant fraction in human umbilical vein endothelial cells. *Thromb.Res.* 97 (2000) 505-511.

[30] Vielma, S., Virella, G., Gorod, A., Lopes-Virella, M., Chlamydophila pneumoniae infection of human aortic endothelial cells induces the expression of FC gamma receptor II (FcgammaRII). *Clin.Immunol.* 104 (2002) 265-273.

[31] Mishima, T., Kurasawa, G., Ishikawa, G., Mori, M., Kawahigashi, Y., *et al.*, Endothelial expression of Fc gamma receptor IIb in the full-term human placenta. *Placenta* 28 (2007) 170-174.

[32] Arvidsson, S., Askendal, A., Tengvall, P., Blood plasma contact activation on silicon, titanium and aluminium. *Biomaterials* 28 (2007) 1346-1354.

[33] Hartwig, J. H., Stossel, T. P., Interactions of actin, myosin, and an actin-binding protein of rabbit pulmonary macrophages. III. Effects of cytochalasin B. *J.Cell Biol.* 71 (1976) 295-303.

[34] Stockem, W., Hoffmann, H. U., Gruber, B., Dynamics of the cytoskeleton in Amoeba proteus. I. Redistribution of microinjected fluorescein-labeled actin during locomotion, immobilization and phagocytosis. *Cell Tissue Res.* 232 (1983) 79-96.

[35] Falcone, S., Cocucci, E., Podini, P., Kirchhausen, T., Clementi, E., *et al.*, Macropinocytosis: regulated coordination of endocytic and exocytic membrane traffic events. *J.Cell Sci.* 119 (2006) 4758-4769.

[36] Hartig, S. M., Greene, R. R., Carlesso, G., Higginbotham, J. N., Khan, W. N., *et al.*, Kinetic analysis of nanoparticulate polyelectrolyte complex interactions with endothelial cells. *Biomaterials* 28 (2007) 3843-3855.

[37] Loubery, S., Wilhelm, C., Hurbain, I., Neveu, S., Louvard, D., *et al.*, Different Microtubule Motors Move Early and Late Endocytic Compartments. *Traffic* 9(4) (2008) 492-509.

[38] Slowing, I. I., Trewyn, B. G., Lin, V. S., Mesoporous silica nanoparticles for intracellular delivery of membrane-impermeable proteins. *J.Am.Chem.Soc.* 129 (2007) 8845-8849.

[39] Fadok, V. A., Voelker, D. R., Campbell, P. A., Cohen, J. J., Bratton, D. L., *et al.*, Exposure of phosphatidylserine on the surface of apoptotic lymphocytes triggers specific recognition and removal by macrophages. *J.Immunol.* 148 (1992) 2207-2216.

[40] Dickson, J. S., Koohmaraie, M., Cell surface charge characteristics and their relationship to bacterial attachment to meat surfaces. *Appl.Environ.Microbiol.* 55 (1989) 832-836.

Acknowledgements: We wish to thank Angelo Benedetto and the Rice Shared Resource Facility for training in scanning electron microscopy (SEM) and Kenneth Dunner Jr. at MD Anderson Cancer Research Center for sample processing and image analysis by transmission electron microscopy. We also thank Matt Landry for aid in assembling high resolution figures for publication and Kathryn Hodges for technical assistance. This research was supported by grants DODW81XWH-07-1-0596 and DODW81XWH-04-2-0035; NASA Grant #SA23-06-017; and State of Texas, Emerging Technology Fund.

FIGURE LEGENDS

Fig. 1. Microparticle surface charge and binding by serum opsonins directs uptake by HUVECs. (**A**) SEM images of non-serum opsonized silicon microparticle internalization by HUVECs. Negative (oxidized), positive (APTES), and mPEG-5000 modified microparticles were incubated with HUVECs for 60 min at 37ºC. (**B**) Flow cytometry analysis of microparticle (MP) uptake by HUVECs in serum-free or serum-containing media (* $p = 0.0004$; ** $p = 0.015$). (**C**) Electrostatic (zeta) potential of microparticles before and after serum opsonization (60 min, 4ºC). (**D**) Flow cytometry analysis of microparticle uptake by J774 cells in serum-free or serum-containing media (* $p = 0.03$). (**E,F**) Flow cytometry analysis of non-serum opsonized vs IgG-opsonized oxidized microparticle uptake by HUVEC (**E**) and J774 (**F**) cells.

Fig. 2. Inflammatory cytokines stimulate silicon microparticle uptake by HUVECs. (**A,B)** Flow cytometry analysis of silicon microparticle uptake by HUVEC (**A**) and J774 (**B**) cells in the presence of 2% serum before and after cytokine (TNF-α and IFN-γ) stimulation for 48 hrs (* $p = 0.045$). (**C,D**) SEM images of silicon microparticle uptake by HUVEC (**C**) and J774 (**D**) cells (30 min, 37ºC).

Fig. 3. Internalization of oxidized silicon microparticles by HUVECs. (**A**) SEM images of HUVECs after incubation with either 1.6 µm, 3.2 µm, or both sizes of oxidized silicon microparticles at 37ºC for 15 min, 30, or 60 min in serum-free media. (**B,C**) Confocal micrographs of HUVECs incubated with 3.2 µm oxidized silicon microparticles for 5 and 120 min at 37ºC using Alexa Fluor 555 Phalloidin for actin staining. (**C**) Confocal projection images cropped through the center to illustrate microparticle location in HUVECs over time.

Fig. 4. Cytochalasin B blocks microparticle uptake by HUVECs. (**A**) SEM images of HUVECs incubated with 1.6 µm and 3.2 µm oxidized silicon particles at 37ºC for 15 and 30 min in serum-free media containing 2.5 µg/ml Cytochalasin B. (**b**B Confocal micrographs of Cytochalasin B treated HUVECs incubated with 3.2 µm microparticles for 60 min and stained with FITC conjugated anti-tubulin antibody and Alexa Fluor 555 Phalloidin. (**C**) Flow cytometric analysis showing orthogonal 90º laser light scatter by HUVECs before (left) and after incubation with silicon microparticles (right). (**D**) Side scatter was used as a metric for HUVEC uptake of microparticles treated with increasing concentrations of Cytochalasin B.

Fig. 5. Early uptake of oxidized silicon microparticles and FITC dextran by HUVECs. TEM analysis showing HUVEC uptake of either 1.6 µm (**A**) or 3.2 µm (**B**) silicon particles after incubation at 37ºC for 15 min. (**C**) Flow cytometric analysis of FITC dextran internalization by HUVECs incubated for 1 hr with none (green), 1.6 µm (red) or 3.2 µm (purple) silicon particles. The solid blue peak represents HUVECs incubated in media without FITC dextran.

Fig. 6. Trafficking of oxidized silicon microparticles in HUVECs. HUVECs were incubated with oxidized silicon microparticles for 120 min at 37ºC. (**A,B**) TEM images of cells with internalized 1.6 µm (**A**) or 3.2 µm (**B**) particles. (**C**) Confocal micrographs of HUVECs containing internalized DyLight 488 labeled silicon microparticles. Acidic vesicles were stained with Lysotracker Red and nuclei were stained with 4',6-diamidino-2-phenylindole (DAPI).